# High-Concentration Dispersion of Single-Wall Carbon Nanotubes

**Y. Sabba and E. L. Thomas***

*Department of Materials Science and Engineering, Massachusetts Institute of Technology, Cambridge, Massachusetts 02139*

*Received February 12, 2004; Revised Manuscript Received April 25, 2004*

ABSTRACT: We report a novel method to exfoliate and disperse single-wall carbon nanotubes (SWNT) into organic and aqueous solutions. The method is based on treatment of single-wall carbon nanotubes with a solution of hydroxylamine hydrochloric acid salt [($NH_2OH$)(HCl)] and does not require truncation of the tubes or surface adsorption of organic molecules. The solution dispersed tubes can easily be incorporated into an organic matrix in order to obtain a nanocomposite. We illustrate the method by forming PMMA−SWNT and PS−SWNT nanocomposites. 1% SWNT PMMA nanocomposite having a draw ratio of ∼6 showed a dramatic 7× increase in the strain to fracture compared to fibers of similar draw ratio made from pure PMMA.

## Introduction

Dispersion of single-wall carbon nanotubes (SWNT) is an important first step toward many potential applications that harness the unique electronic, thermal, optical, and mechanical properties of the individual tube.[1−13] Furthermore, conventional applications such as the use of SWNT as conductive fillers in composites will benefit from a well-dispersed system that will exhibit the same conductivity with a smaller percentage of filler. Well-dispersed SWNT in a particular solvent are also the preferred state for chemical modification of SWNT.

As a result of the substantial van der Waals attraction (∼950 meV/nm), nanotubes tend to aggregate easily and are difficult to suspend.[14] SWNT can be suspended in concentrated strong acids such as 102% $H_2SO_4$ to form a nematic liquid crystal solution;[18] however, the acid tends to digest the tubes[15−18] and reduce their length. The resultant short fragments, ∼100 nm in length, do not entangle, and the overall van der Waals force for a single tube ($F \sim f(l)$) is substantially lower. Such fragments can be suspended in water and organic solvents.[15,16] Short fragments of nanotubes have an aspect ratio that is more than an order of magnitude lower than that of original tubes. Since it is often advantageous to use high aspect ratio nanotubes in various applications, it is worthwhile to develop a dispersion process that does not significantly shorten the tubes.

Chemical modification of the SWNT is another method to obtain a stable dispersion in organic media.[19−24] Other "nondestructive" methods for dispersion of SWNT such as absorbing polymers and surfactants onto the nanotube surface are common methods to obtain a stable organic or aqueous SWNT dispersion.[18,25−31] The dispersion via adsorption of surfactant molecules approach has the disadvantage in that the molecules that remain on the surface of the nanotubes may reduce compatibility with the host matrix material. Moreover, the maximum concentration that can be dispersed in a solution is only about 1%.

* Corresponding author. E-mail: elt@mit.edu.

## Thermodynamics of SWNT in Solution

SWNT can be viewed as needlelike objects having a very large aspect ratio. The dispersion vs aggregation of needlelike objects can be understood using Onsager's theory for electrostatic repulsion of lengthy anisotropic particles.[31] The free energy of a dilute system (the isotropic phase) ($\phi \ll 1$, $\phi$ is the volume fraction) of long rodlike particles ($l \gg d$) of polydisperse lengths $l_1, ..., l_s, ...$ but having identical diameter $d_1 = d_2 = ... = d_s = d$ relative to the pure solvent is given by[32,33]

$$F = F(\text{solution}) - F(\text{solvent}) = F_0 - kT \log(B_p(N_p,V,T)) \quad (1a)$$

$$F_0 = N_p\mu_0,$$

$$\log(B_p) = \sum_s N_s(1 + \log(\nu/N_s)) - \frac{(\pi(d + \bar{\delta}))}{4V}\sum_{s,s'} N_s N_{s'} l_s l_{s'} \quad (1b)$$

where $F_0$ is the free energy component that depends only on temperature, $B_p = \int(\exp(-w/kT)\, d\tau/N_p!)$ is the configuration integral for the particles, $w$ stands for the interparticle potential of the average forces that act between the particles (Onsager takes a repulsive potential $w \geq 0$), $d\tau$ denotes a volume element in configuration space, $N_p$ is the total number of particles in the solution, $N_s$ is the total number of particles of length $l_s$, and $V$ is the volume of the solution. The potential of the average force that is generated by the ionic double layer decays exponentially with the distance and can be considered as an effective increase in the diameter of the particle from $d$ to $d + \bar{\delta}$.

The chemical potential of a rod of length $l_s$ is given by

$$\mu_s = \left(\frac{\partial F}{\partial N_s}\right) = \mu_s^0(T,\text{solvent}) + kT \log(N_s/V) + 2kT\left(\frac{\pi}{4}\right)(d + \bar{\delta})l_s\left(\frac{L}{V}\right) \quad (2)$$

where $L$ is the sum of the lengths of all particles present, $L = \sum_s N_s l_s$.

10.1021/ma049706u CCC: $27.50 
Published on Web 06/02/2004

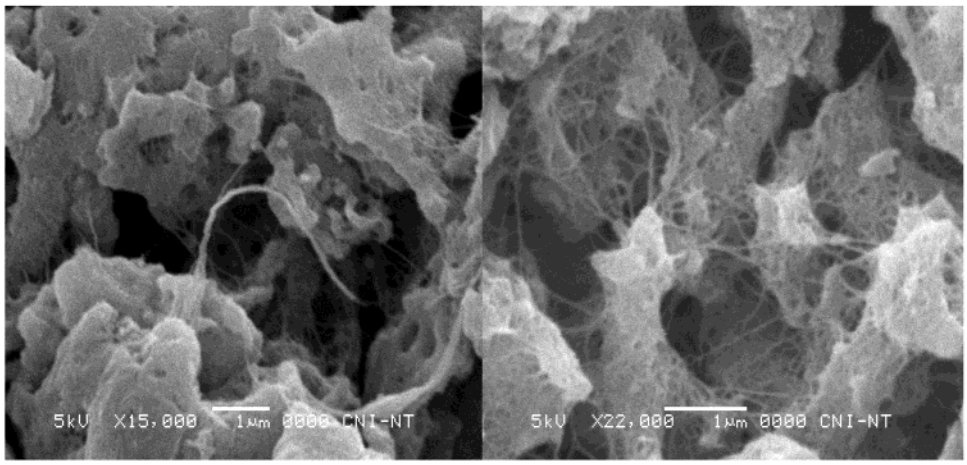


**Figure 1.** SEM images of a pristine, as-received, CNI-purified SWNT.

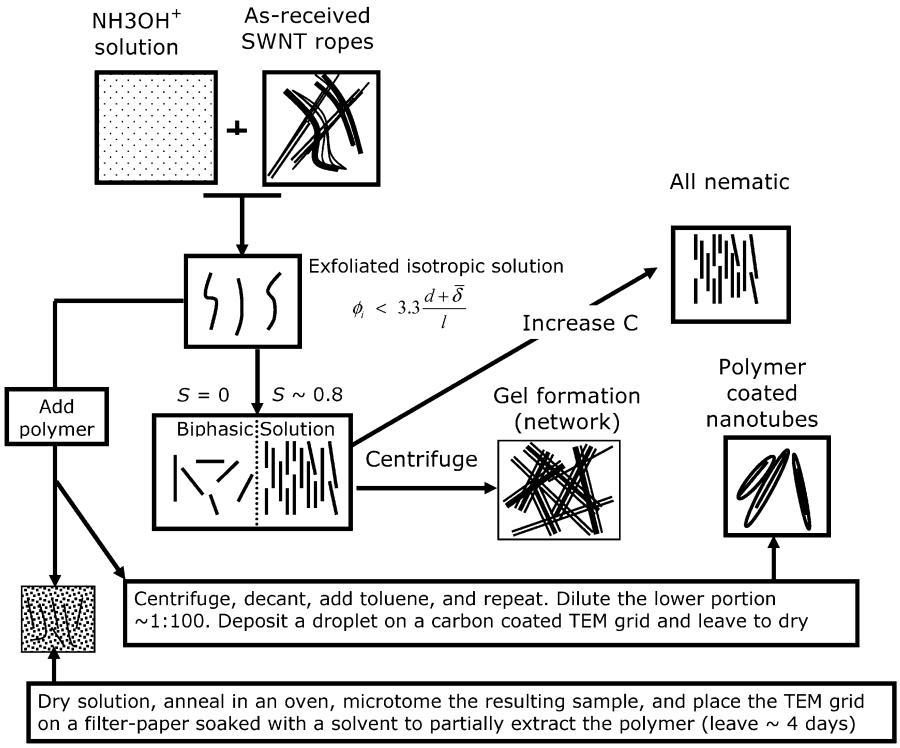


**Figure 2.** Schematic describing exfoliation and nanocomposite formation.

The entropy of mixing is then

$$S = \left(\frac{\partial F}{\partial T}\right)_{N_p,V,P} = N_p \frac{\partial \mu_0}{\partial T} - \left(k \log(B_p) + kT \frac{\partial}{\partial T} \log B_p\right) = N_p \frac{\partial \mu_0}{\partial T} - k \log(B_p) \quad (3)$$

Thus, the entropy of mixing per rod of length $l_s$ is

$$\frac{\partial S}{\partial N_s} = \frac{\partial \mu_0}{\partial T} + k \log(N_s/V) + 2k\left(\frac{\pi}{4}\right)(d + \bar{\delta}) l_s \left(\frac{L}{V}\right) \text{ at } \phi < 1,$$

$$\frac{\partial S}{\partial N_s} \approx \frac{\partial \mu_0}{\partial T} + k \log(N_s/V) \quad (4)$$

The energy of mixing $E$ is then simply

$$E = F - TS = N_p\left(\mu_0 - T \frac{\partial \mu_0}{\partial T}\right) \gg 1 \quad (5)$$

The entropy increases with the number of rods at the rate given by eq 4.

For nanotubes in solution the interparticle potential $w$ is attractive due to the large van der Waals forces and the lack of an inherently good solvent for nanotubes. $E$ is therefore large and positive, and thus only when $N_s/V \rightarrow 0$ is the free energy of mixing negative. This means that only extremely dilute solutions of nanotubes are thermodynamically favorable.

Onsager predicts that the rod−solvent system forms an anisotropic nematic phase at a volume fraction of $\phi_i^c \approx 3.3d/l$, with the volume fraction of the tubes in the

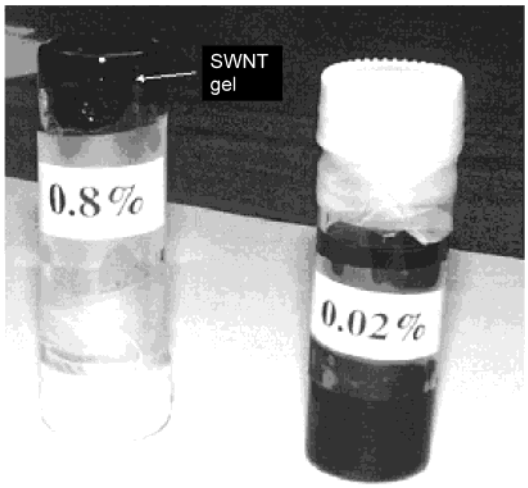


**Figure 3.** Dispersed SWNT in THF. Two concentrations are shown; the upside-down vial on the left contains a 0.8 wt % SWNT in THF. Because of the high viscosity, the solution does not flow. The vial on the right contains a dilute isotropic solution of SWNT in THF, $C \sim 0.02$ wt %.

nematic phase in equilibrium given by $\phi_n^c \approx 4.5d/l$. For SWNT, $d \sim 10^{-9}$m and $l \sim 10^{-6}$ m; thus, the weight fraction of the rods at the transition is $\sim 10^{-3}$. The order parameter $S_c$ in the nematic phase just at the transition is $S_c \approx 0.8$.[37] This value is quite large and indicates an abrupt transition between an isotropic phase $S = 0$ and a highly ordered nematic phase.[37] Consequently, the nanotubes aggregate to form ropes due to the high van der Waals forces between the SWNT, their proximity, and their high alignment in the nematic phase.

From the above discussion a good strategy to disperse SWNT is to create a repulsive interrod potential and increase the ratio between the tube diameter and length. Both these effects can be simultaneously achieved by charging the tubes.

## Experimental Section

Both Carbolex Inc. AP grade and Carbon Nanotechnologies Inc. (CNI) purified (>95% pure) grade SWNT's were used. As-received samples consist of SWNT ropes. Figure 1a,b shows SEM images of the pristine as-received nanotubes in which the ropes are clearly visible.

The SWNT were treated with a 10 wt % solution of $(NH_2OH)(HCl)$ in deionized water for 24 h. In water, $(NH_2OH)(HCl)$ will dissociate into $NH_3OH^+$ and $Cl^-$ to form an acidic solution.[40] Owing to its acidic nature, $NH_3OH^+$ will have good affinity for surfaces with high electron densities and, thus, is expected to readily adsorb on nanotube surfaces.

Furthermore, the small size of this cation enables it to easily impregnate and diffuse through the spaces between the individual tubes (measured as $d = 2.4$ Å[33]) that make up the nanotube ropes. Ultimately, the cation induces a positive charge on the individual nanotubes, which results in a repulsive interaction between neighboring tubes. This repulsive force is capable of overcoming the attractive, van der Waals force between the tubes and thus enables the exfoliation of the ropes. In addition, the repulsive interaction increases their effective diameter, thus preventing the dispersed tubes from reagglomerating.

The SWNT/$(NH_2OH)(HCl)$ solution was then centrifuged and the clear upper portion decanted. The viscous lower fraction has a tube concentration of about 1−2 wt %. This fraction was then washed several times with pure deionized water in order to remove any traces of salt. The tubes were then washed several times with THF to exchange $H_2O$ to THF as the solvent (Figure 2).

The resulting SWNT/THF suspension has a concentration of 1−2 wt % of nanotubes. At this concentration the solution viscosity is extremely high, and thus a gel is formed (Figure 3a). The high viscosity is observed even at a solution concentration of 0.5 wt %.Figure 4 shows images of two nanocomposite films prepared by blending PMMA, MW 45 000 and PDI 1.9 (Figure 4a,b), or PS, MW 100 000 (Figure 4c,d), with the SWNT THF solution. These samples were prepared by adding a dispersion of SWNT in THF to a PS−THF or PMMA−THF solution. The solution was precipitated in methanol, dried, and annealed 12 h in a vacuum oven at temperatures of ∼130−170 °C. A fragment of the sample was embedded in a Spurr epoxy resin and then sectioned using an ultramicrotome. The sections were collected on a lacy carbon-coated TEM copper grid. The grids were then placed on a filter paper soaked with solvent (DMF for PMMA and toluene for the PS) in order to leach out some of the polymer and thus further thin the sections and enhance the visibility of the individual nanotubes.

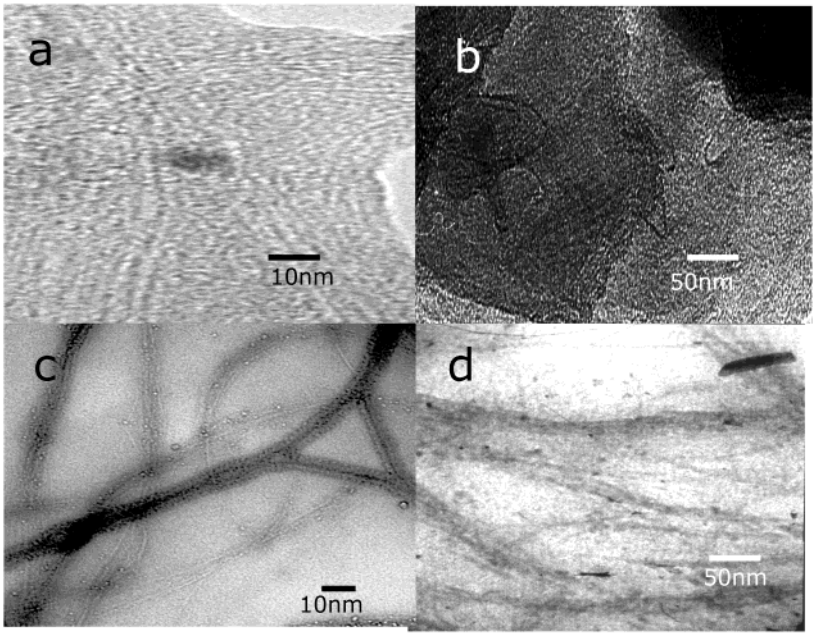


**Figure 4.** TEM images of a dispersed SWNT nanocomposite: (a, b) PMMA−SWNT nanocomposite; (c, d) PS−SWNT nanocomposite.

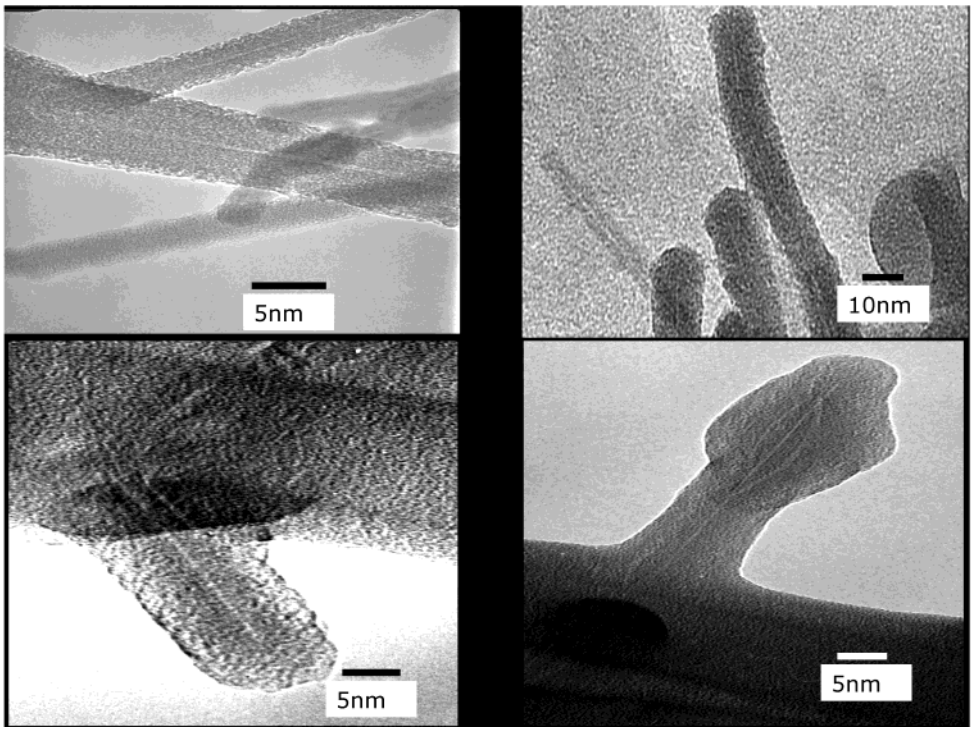


**Figure 5.** TEM micrographs of PS-coated SWNT.

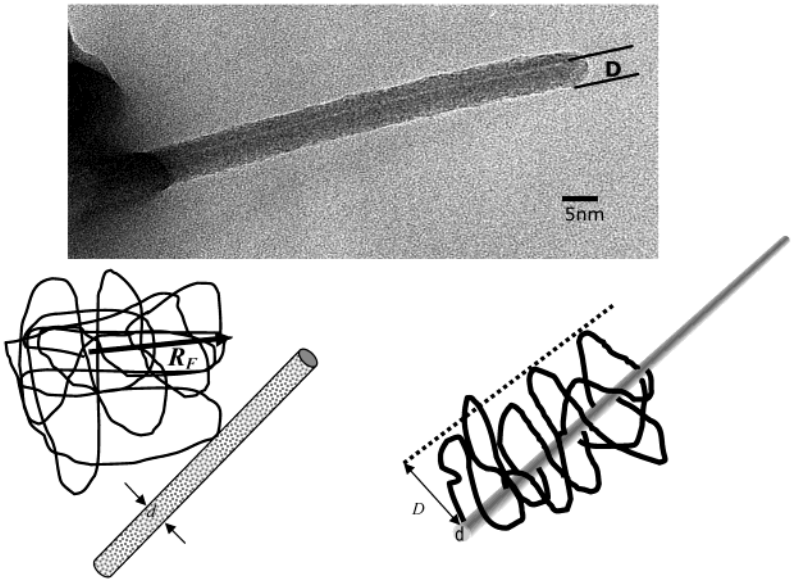


**Figure 6.** TEM image of the confined PS layer on a SWNT.

Another method of sample preparation was to centrifuge the PS/SWNT solution in THF and decant the upper fraction. The lower fraction was washed with toluene and centrifuged again twice. A droplet of the lower fraction was placed on a lacy carbon-coated TEM cupper grid and allowed to dry. TEM images from these samples (Figure 5) show individual tubes coated with a layer of adsorbed PS.

## Results and Discussion

By inspection of the TEM images such as Figure 6, the thickness of the adsorbed layer is about 5−10 nm. Pincus et al. suggest that the thickness $D$ of the adsorbed layer of polymer on a cylindrical colloidal particle is given by[35]

$$D \sim d \exp(\epsilon_t/\epsilon) \qquad (6)$$

where $d$ is the colloidal rod diameter, $\epsilon k_B T$ is the amount in the free energy reduction of monomers within the adsorbing layer, and $\epsilon_t k_B T \sim (a/d) k_B T$ is the minimum reduction of free energy required for a segment of length $a$ to adsorb. In solution, the coil's end-to-end distance is $R_g = R_F \approx aN^{3/5} \sim 100$ nm, the diameter of the nanotube $d \sim 1-3$ nm, and the polymer segment $a \sim 1$ nm. For van der Waals attraction between the chain and the surface $\epsilon \sim 10^{-1}$, and thus $D \sim 100$ nm for the swollen adsorbed polymer layer; thus, the adsorbed chain is distorted from its normal size and shape in a good solvent. Such distortion costs elastic energy[36] which is compensated by maximizing the number of contacts with the surface—a process known as "escape upon the surface".[35,38]

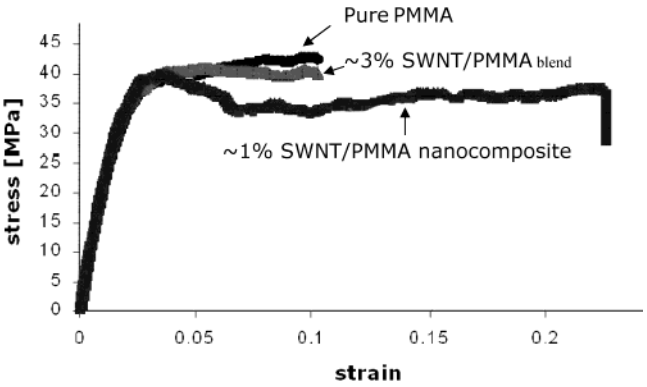


**Figure 7.** Stress−strain curves of pure PMMA, a 3% PMMA/SWNT blend, and a ~1% PMMA/SWNT nanocomposite.

It should be noted that eq 5 describes the adsorption of a single chain; in our case, a SWNT has a radius $d \sim 1$ nm and length $l \sim 10^3$nm so the total surface area that is available for adsorption is $S_{nt} \sim 10^{-15}$ m$^2$, while the aerial dimension of a polymer segment is roughly $\sim a^2$. For $a \sim 1$ nm, the surface that is taken by a segment is approximately $s_{seg} \sim 10^{-18}$ m$^2$; thus, the maximum number of segments that can be adsorbed on to the surface of a 1 $\mu$m long SWNT is $<10^3$. This is approximately the number of segments of the PS chain that was used (MW = 100 000). Thus, our assumption of a single-chain adsorption on an individual SWNT is reasonable. The swollen chain is expected to shrink when the solvent evaporates leaving a dry layer that is at least[36,39] $aN^{3/5}/aN^{1/2} = N^{1/10}$ (~2.5 for $N \sim 100\,000$) thinner than the swollen chain. In addition, because of the aromatic nature of styrene, the interaction between the PS segment and the SWNT is expected to be more then a simple van der Waals interaction. A consequence of this is that the reduction of free energy of an adsorbed PS segment is expected to be lower than $10^{-1}k_BT$, and this will further decrease the swollen layer thickness $D$. Thus, the PS layer thickness surrounding the SWNTs observed in Figures 5 and 6 is in reasonable agreement with the calculated one.

To explore the mechanical properties of polymer−SWNT nanocomposites, a HAAKE MiniLab counter−rotating miniextruder rotating at 200 rpm was employed in order to produce ~100 $\mu$m diameter fibers of PMMA, of ~3% (as received) SWNT−PMMA blends, and the exfoliated ~1% SWNT−PMMA nanocomposite. Fibers having a draw ratio of approximately 6, based on the square of the die diameter to fiber diameter, were produced after 5 min of recirculation of the materials. The relative mechanical behavior of these specimens, tested at an elongation rate of 10 mm/min at room temperature, is shown in Figure 7. As is evident from the strain−stress curve, the modulus and yield strength of all three materials are approximately equal. However, the exfoliated 1% SWNT−PMMA nanocomposite produced via the hydroxylamine hydrochloric acid salt method shows a dramatic increase in the strain to fracture compared to the average value of 0.1 for the PMMA to approximately 0.7 for the 1% SWNT−PMMA nanocomposite, suggesting a marked change in the mechanical behavior of the well-dispersed nanotube polymer system. We are continuing to characterize the degree of orientation and other physical properties of the nanocomposites.

We have also demonstrated SWNT−polymer nanocomposites with concentrations of up to ~10−20% SWNT, adding a small amount of polymer to a large volume of a 1% SWNT solution created via the [$NH_2$-OH]HCl method and precipitating in methanol then reswelling with THF, followed by adding more SWNT suspension and reprecipitation in methanol.

## Conclusions

By considering Onsager's thermodynamic treatment of needlelike objects in solution, we have demonstrated a dispersion method that does not involve the truncation or digestion of SWNT. Dispersion is achieved by inducing an electric charge on the SWNT, and the electrostatic repulsion reduces the overall forces that hold the tubes together in ropes. A polymer/SWNT nanocomposite can be easily obtained by directly blending the SWNT dispersion with any polymer solution, such as PMMA, PS, polyisocyanate, hydroxypropylcellulose, and poly(ethylene glycol).

**Acknowledgment.** This research was sponsored by the Cambridge MIT Institute.

## References and Notes

(1) Dresselhaus, M. S.; Dresselhaus, G.; Eklund, P. C. *Science of Fullerenes and Carbon Nanotubes*; Academic Press: San Diego, CA, 1996.
(2) Saito, R.; Dresselhaus, M. S. *Physical Properties of Carbon Nanotubes*; Imperial College Press: London, 1998.
(3) Odom, T. W.; Huang, J. L.; Kim, P.; Lieber, C. M. *Nature (London)* **1998**, *391*, 62.
(4) McEuen, P. L. *Phys. World* **2000**, *6*, 31.
(5) Smith, B. W.; Benes, Z.; Luzzi, D. E.; Fischer, J. E.; Walters, D. A.; Casavant, M. J.; Schmidt, J.; Smalley, R. E. *Appl. Phys. Lett.* **2000**, *77*, 663.
(6) Hone, J.; Llaguno, M. C.; Nemes, N. M.; Johnson, A. T.; Fiscer, J. E. Walters, D. A.; Casavant, M. J. Smalley, R. E. *Appl. Phys. Lett.* **2000**, *77*, 666.
(7) Mintmire, J.; W. White, C. T. *Carbon* **1995**, *33*, 893.
(8) Li, F.; Cheng, B. S.; Su, G.; Dresselhaus, M. S. *Appl. Phys. Lett.* **2000**, *77*, 663.
(9) Dekker, C. *Phys. Today* **1999**, *52*, 22.
(10) Wong, E. W.; Sheehan, P. E.; Lieber, C. M. *Science* **1997**, *277*, 1971.
(11) Fan, S.; Chapline, M. G.; Franklin, N. R.; Tombler, T. W.; Cassell, A. M.; Dai, H. *Science* **1999**, *283*, 512.
(12) Kong, J.; Franklin, N.; Zhou, C.; Chapline, M,; Peng, S.; Cho, K.; Dai, H. *Science* **2000**, *287*, 622.
(13) de Heer, W. A.; Bacsa, W. S.; Chatelain, A.; Garfin, T.; Humphrey-Baker, R.; Forro, L.; Ugarte, D. *Science* **1995**, *268*, 845.
(14) Girifalco, L. A.; Hodak, M.; Lee, R. S. *Phys. Rev. B* **2000**, *62*, 13104.
(15) Bahr, J. L.; Mickelson, E. T.; Bronikowski, M. J.; Smalley, R. E.; Tour, J. *Chem. Commun.* **2001**, *2*, 193.
(16) Ausman, K. D.; Piner, R.; Lourie, O.; Ruff, R. R.; Korobov, M. *J. Phys. Chem. B* **2000**, *104*, 8911.
(17) Liu, J.; Rinzler, A. G.; Dai, H. J.; Hafner, J. H.; Bradley, R. K.; Boul, P. J.; Lu, A.; Iverson, T.; Shelimov, K. Huffman, C. B.; Rodriguez-Marcias, F. J.; Shon, Y. S.; Lee, T. R.; Colbert, D. T.; Smalley, R. E. *Science* **1998**, *280*, 1253.
(18) Davice, V. A.; Ericson, L. M.; Parra-Vasquez, A. N. G.; Fan, H.; Wang, Y.; Prieto, V.; Longoria, J. A.; Ramesh, S.; Saini, R. K.; Kittrell, C.; Billups, W. E.; Adams, W. W.; Hauge, R. H.; Smally, R. E.; Pasquali, M. *Macromolecules* **2004**, *37*, 154.
(19) Chen, R. J.; Zhang, Y.; Wang, D.; Dai, H. *J. Am. Chem. Soc.* **2001**, *123*, 3838.
(20) Chen, J.; Hamon, M. A.; Hu, H.; Chen, Y.; Rao, A. M.; Eklund, P. C.; Haddon, R. C. *Science* **1998**, *282*, 95.
(21) Kahn, M. G. C.; Banerjee, S.; Wong, S. S. *Nano Lett.* **2002**, *2*, 1215.
(22) Sano, M.; Kamino, A.; Okamura, J.; Shinkai, S. *Langmuir* **2001**, *17*, 5125.
(23) Nakashima, N.; Tomonari, Y.; Murakami, H. *Chem. Lett.* **2002**, 638.
(24) Pompeo, F.; Resasco, D. E. *Nano Lett.* **2002**, *2*, 369.
(25) Selimov, K. B.; Rint, R. O.; Rinzler, A. G.; Huffman, C. B.; Smalley, R. E. *Chem. Phys. lett.* **1998**, *282*, 429.

(26) Bandow, S.; Rao, A. M.; Williams, K. A.; Thess, A.; Smalley, R. E.; Eklund, P. C. *J. Phys. Chem. B* **1997**, *101*, 8839.
(27) Duesberg, G. S.; Burghard, M.; Muster, J.; Philipp, G.; Roth, S. *Chem. Commun.* **1998**, *3*, 453.
(28) O'Connell, M. J.; Boul, P.; Ericson, L.; Huffman, C.; Wang, Y.; Haroz, E.; Kuyper, C.; Tour, J.; Ausman, K. D.; Smalley, R. E. *Chem. Phys. Lett.* **2001**, *342*, 265.
(29) Star, A.; Steuerman, D. W.; Heath, J. R.; Stoddart, J. F. *Angew. Chem., Int. Ed.* 2**002**, *41*, 2508.
(30) Bandyopadhyaya, R.; Nativ-Roth, E.; Regev, O.; Yerushalmi-Rozen, R. *Nano Lett.* **2002**, *2*, 25.
(31) Islam, M. F.; Rojas, E.; Bergey, D. M.; Johnson, A. T.; Yodh, A. G. *Nano Lett.* **2003**, *3*, 269.
(32) Onsager, L. *Ann. N.Y. Acad. Sci.* **1949**, *51*, 627.
(33) Hill, T. L. *Statistical Thermodynamics*; Addison-Wesley Publishing Co.: Reading, MA, 1960.
(34) Schlittler, R. R.; Seo, J. W.; Gimzewski, J. K.; Durkan, C.; Saifullah, M. S. M.; Welland, M. E. *Science* **2001**, *292*, 1136.
(35) Pincus, P. A.; Sandroff, C. J.; Witten, T. A., Jr. *J. Phys. (Paris)* **1984**, *45*, 725.
(36) De Gennes, P. G. *Scaling Concepts in Polymer Physics*; Cornell University Press: Ithaca, NY, 1979.
(37) De Gennes, P. G.; Prost, J. *The Physics of Liquid Crystals*, 2nd ed.; Oxford Science Publications: New York, 1993.
(38) De Gennes, P. G. *Macromolecules* **1981**, *16*, 1637.
(39) Brochard, F.; De Gennes, P. G. *Macromolecules* **1977**, *10*, 1157.
(40) Ritz, J.; Fuchs, H.; Perryman, H. In *Ullmann's Encyclopedia of Industrial Chemistry*; Wiley-VCH: New York, 2004.

MA049706U